IEEE JOURNAL OF SELECTED TOPICS IN QUANTUM ELECTRONICS, VOL. 11, NO. 5, SEPTEMBER/OCTOBER 2005

Nearly Diffraction Limited 980-nm Tapered Diode Lasers With an Output Power of 7.7 W

Katrin Paschke, Bernd Sumpf, Frank Dittmar, Götz Erbert, *Member, IEEE*, Ralf Staske, Hans Wenzel,
and Günther Tränkle, *Member, IEEE*

***Abstract*—High-brightness tapered diode lasers emitting at 980 nm with electrically separated straight ridge waveguide and tapered gain-guided sections were fabricated. An output power of more than 14 W was achieved in quasi-continuous wave (QCW) operation. The value of the beam propagation ratio M^2 remained below 2 up to a power of 7.7 W if the sections were separately contacted. The vertical beam divergence was 18° (FWHM) only.**

***Index Terms*—Beam quality, high brightness, high-power laser, semiconductor laser, tapered laser.**

I. INTRODUCTION

DIODE lasers with high output power and high beam quality are required for many commercial and scientific applications. One of the most promising devices are tapered diode lasers which consist of a straight ridge waveguide (RW) section and a tapered gain-guided section. For a wide wavelength range this approach has been successfully tested and output powers up to 5 W were achieved [1]–[6].

We investigated experimentally the dependence of the beam quality of 735 nm tapered lasers on different geometrical parameters such as the lengths of the RW and tapered sections in [7]. In this paper, we present experimental data suitable for a better understanding of the impact of the current injected into RW section on output power and beam quality which will give design rules for a further optimization of 980-nm tapered lasers. In the tapered devices under study the current through the RW and the tapered sections can be adjusted separately which allows an independent control of output power and beam quality and moreover a simplified modulation of the output power. The RW section was driven in continuous wave (CW) operation, whereas the tapered section was operated with μs current pulses.

In Section II, details of the device structure and the fabrication process will be given. In Section III, the dependence of the output power and beam quality upon the current through the RW and tapered sections will be presented. Finally, conclusions will be given in Section IV.

II. DEVICE STRUCTURE AND FABRICATION

A schematic view of the tapered laser under study is shown in Fig. 1. The vertical laser structure grown by metal-organic chemical vapour phase epitaxy consists of a super large optical cavity (SLOC) with a very broad 3.6-μm-thick $\mathrm{Al}_{0.45}\mathrm{Ga}_{0.55}\mathrm{As}$ waveguide embedded in $\mathrm{Al}_{0.70}\mathrm{Ga}_{0.30}\mathrm{As}$ cladding layers. The thickness of the cladding layers is optimised for minimal series resistance and fundamental-mode radiation losses. The active region is composed of a compressively strained InGaAs single quantum well sandwiched between tensile-strained GaAsP barriers. This SLOC structure not only reduces the facet load but also results in an excellent small vertical far field angle of 18.4° (full width half maximum), and about 96% of the output power is included within a vertical far field angle of only 33.6° as shown in Fig. 2. The internal efficiency is larger than 95% and the internal losses are about 1.4 cm^{-1}, both value determined from an analysis of the cavity-length dependence of threshold current and external differential efficiency of equivalent broad area (BA) lasers.

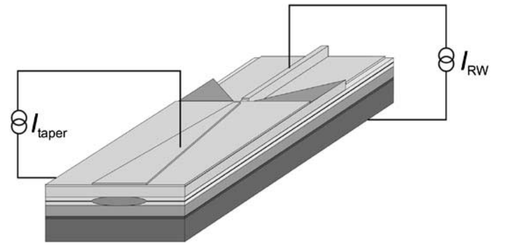

Fig. 1. Schematic three dimensional view of a tapered laser.

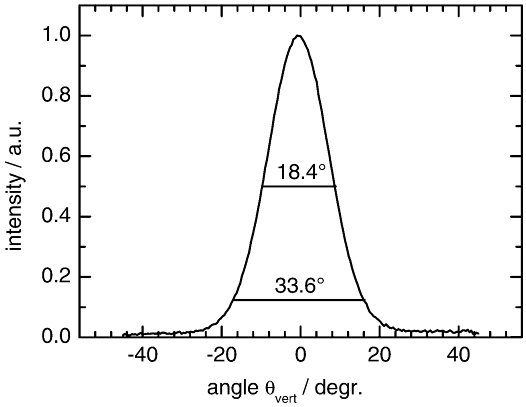

Fig. 2. Profile of vertical far field intensity.

The fabrication of tapered lasers uses a combination of well-established processing steps for RW and BA lasers. A total laser length of $L = 4$ mm was selected to achieve high output power. The RW section is formed by reactive ion etching of a mesa structure.

Manuscript received November 23, 2004. This work was supported by Zukunftsfond Berlin.

The authors are with the Ferdinand-Braun-Institut für Höchstfrequenztechnik, D-12489 Berlin, Germany (e-mail: Katrin.Paschke@fbh-berlin.de; Bernd.Sumpf@fbh-berlin.de; Frank.Dittmar@fbh-berlin.de; Goetz.Erbert@fbh-berlin.de; Ralf.Staske@fbh-berlin.de; Hans.Wenzel@fbh-berlin.de; Guenther.Traenkle@fbh-berlin.de).

Digital Object Identifier 10.1109/JSTQE.2005.853840

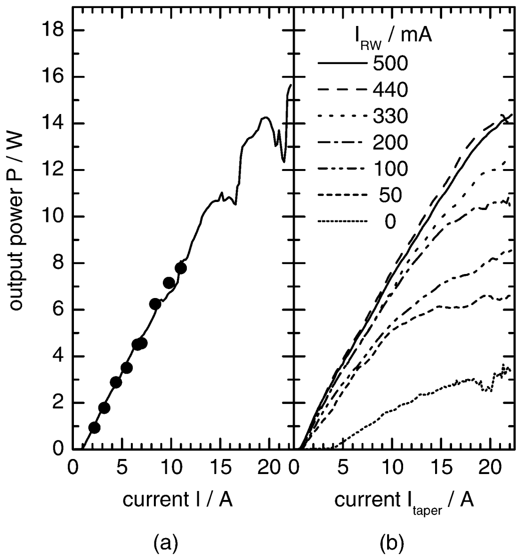

Fig. 3. Light-current characteristics of the tapered diode laser emitting at 980 nm with (a) common (solid line: measurements, bullets: extracted from (b); see text) and (b) separated contacts with the following parameters: $L = 4$ mm, $L_{\mathrm{RW}} = 1350$ μm, $\phi = 6°$, and $R_f = 1\%$. Heat sink temperature $T = 25$ °C.

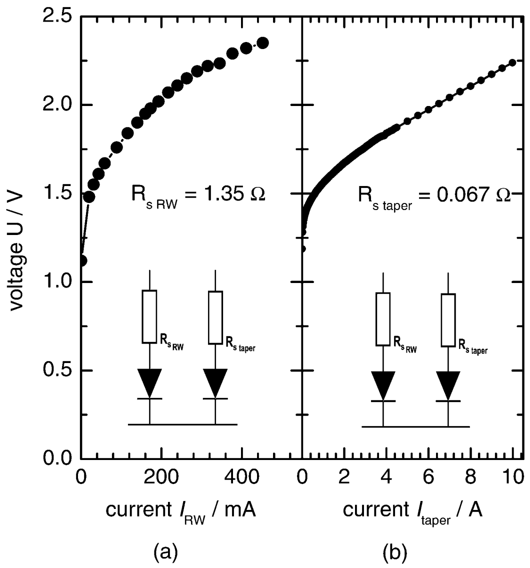

Fig. 4. Voltage-current characteristics for separate contacting of the device in Fig. 3 for (a) RW and (b) tapered sections.

In this paper, we investigate tapered diode lasers with a RW width of $W = 3$ μm and a RW length of $L_{\mathrm{RW}} = 1350$ μm. The etch depth was selected for an appropriate effective index step of $\Delta n_{\mathrm{eff}} = 5 \cdot 10^{-3}$. The tapered section has a length of $L_{\mathrm{taper}} = 2650$ μm and a total flare angle of $\phi = 6°$.

After substrate thinning and depositing the n-metalization, the wafers were cleaved and the facets were anti- and high-reflection coated, respectively $(R_f \approx 1\%, R_r \approx 95\%)$. The devices were finally mounted, junction side up, on standard C-mounts for the measurements.

III. EXPERIMENTAL RESULTS

The output power, the position of the beam waist, the intensity profile in the beam waist, and the lateral far-field profile were measured in dependence on the currents through both sections. Whereas the RW section was driven in CW operation, the tapered section was operated with current pulses of a duration of 10 μs and a repetition rate of 25 Hz. All measurements were performed at a heatsink temperature of $T = 25$ °C.

Fig. 3 shows power-current characteristics of the tapered diode laser with common [Fig. 3(a)] and separated [Fig. 3(b)] contacting. With common contacting and pulsed operation of both sections, at a current of about 22 A a maximum output power of 15 W was achieved. The threshold current was $I_{\mathrm{th}} = 0.98$ A and the measured slope efficiency was $S = 0.78$ W/A. However, for output powers above $P = 10$ W, strong nonlinearities in the light-current characteristic were observed.

In Fig. 3(b), the dependence of the output power upon the current through the tapered section I_{taper} of the same laser, as in Fig. 3(a), is given. The current in the RW section I_{RW} was varied from 0 mA up to 500 mA. With the increase of I_{RW} the slope efficiency of the device increases first from about 0.57 W/A up to 0.77 W/A for $I_{\mathrm{RW}} = 440$ mA and decreases then with a further increase of I_{RW}. For the case $I_{\mathrm{RW}} = 0$, the threshold current is 3.84 A. The highest output power of $P = 14.4$ W was achieved with $I_{\mathrm{RW}} = 440$ mA and $I_{\mathrm{taper}} = 21.2$ A. For this optimal RW current the power-current characteristics remained almost linear within the studied current range. A further increase of the I_{RW} does not lead to an improvement of the output power.

Moreover, Fig. 3(b) illustrates that at constant current in the tapered section the output power can be modulated by a variation of the current through the RW section. This is much easier realized than a modulation of the much larger current through the tapered section.

For a better understanding how the current distributes between the RW and tapered sections in the case of common contacting, the voltage-current characteristics of the RW and tapered sections were measured. The results are shown in Fig. 4(a) and (b), respectively. From these measurements, the serial resistance of the RW and tapered sections $R_{s-\mathrm{taper}}$ and $R_{s-\mathrm{RW}}$, respectively, were estimated to $R_{s-\mathrm{RW}} \approx 1.35$ Ω and $R_{s-\mathrm{taper}} \approx 0.067$ Ω.

Assuming that the current through the tapered laser with common contacting is split like in a parallel circuit, it can be concluded that 95% of the current flows through the tapered section and about 5% through the RW section.

From this, the power-current characteristics for the case of common contacting can be simulated based on the measurements for separate contacting. Using the above results, the bullets in Fig. 3(a) were calculated from Fig. 3(b). The agreement with the directly measured characteristics (solid line) is obvious. This verifies the assumption that the current is divided according to the serial resistances of the two sections.

In the following the lateral beam waist profiles and the lateral far field distribution will be discussed. At first, results for a fixed current $I_{\mathrm{RW}} = 440$ mA will be given. This current corresponds to the optimum value as found above. It yields not only the highest output power, but also the best beam quality at high output powers up to 7.7 W.

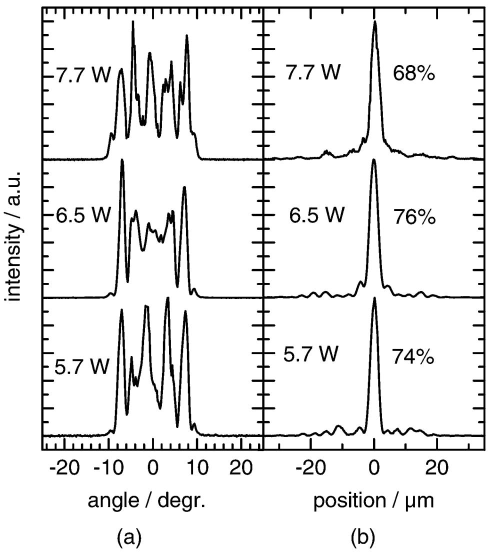

(a) (b)

Fig. 5. Dependence of the (a) lateral far-field profiles and (b) the intensity profiles in the beam waist on output power for the same device as in Fig. 3. The current through the RW section was kept constant to $I_{\mathrm{RW}} = 440$ mA. The relative power in the central lobe P_c is also indicated.

TABLE I
COMPILATION OF BEAM PARAMETERS

P / W	BW / µm	FF / degr.	M^2	P_c / %
5.7	4.5	16.8	1.1	74
6.5	5.1	16.3	1.2	76
7.7	7.2	19.2	1.9	68

Beam waist, far field width and M^2 value were measured at 1/e^2 level. The current through the RW part was $I_{\mathrm{RW}} = 440$ mA.

The results are depicted in Fig. 5(a) and (b), respectively. In Fig. 5(a), the profiles of the far-field intensity are given. There is a slight increase of the far field width (measured at $1/\mathrm{e}^2$ level) with increasing output power. The values are given in Table I. The intensity profiles measured at the beam waist are shown in Fig. 5(b). There are only minor side lobes and with increasing output power the beam waist width increases. Up to an output power $P = 7.7$ W the measured beam waist width ($1/\mathrm{e}^2$ level) is smaller than 7.2 μm. The power included in the central Gaussian-like part is not smaller than 68% in all cases.

The beam parameters are compiled in Table I for separate contacting with the optimal current $I_{\mathrm{RW}} = 440$ mA. A calculation of the beam propagation ratio M^2 from the $1/\mathrm{e}^2$ levels of the intensity profiles of the far-field and beam waist yields even at this high output power values smaller than 2. These small M^2 values illustrate the nearly diffraction limited properties of this laser up to an output power of 7.7 W.

The difference in the beam quality between the case of common and separate contacting is shown in Fig. 6 where the beam propagation ratio M^2 is plotted versus the output power. The solid squares show the results for common contacting, the open circles the results for separate contacting with $I_{\mathrm{RW}} = 440$ mA.

For the case of common contacting up to an output power of $P = 5$ W the M^2 value is close to 1. A further increase of the output power leads to a broadening of the beam width and hence to an increase of M^2. However, above $P = 6$ W, M^2 decreases again and at $P = 6.5$ W there is a minimum with $M^2 = 1.3$. At a larger power the beam quality degrades again.

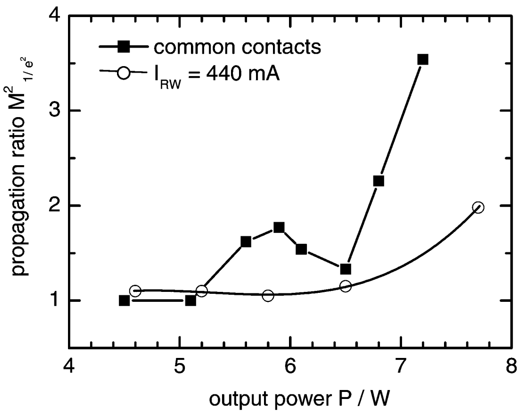

Fig. 6. Dependence of the beam propagation ratio M^2 on the output power for common and separate contacting.

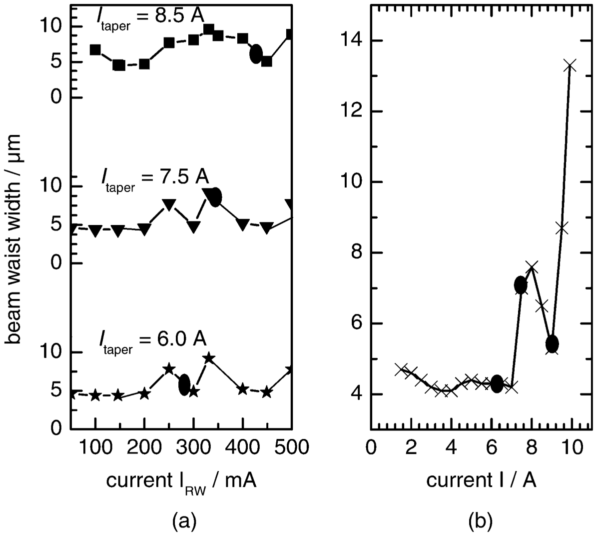

(a) (b)

Fig. 7. Dependence of the beam waist width determined at the $1/\mathrm{e}^2$ level upon the output power with (a) separate and (b) common contacting. In (a), the different curves were shifted for better clarity.

For separate contacting there is a monotonous increase of M^2. But this effect is significantly smaller compared to the case of common contacting, and it demonstrates the advantage of separate contacting.

Finally, it was checked whether the beam waist width in the case of common contacting can also be deduced from the measurements with separate contacting similarly as it was done for the power-current characteristics. For this purpose, measurements of the lateral beam waist width as a function of I_{RW} for three different currents through the tapered section were performed. The results are given in Fig. 7(a). It can be seen, that there is a nonmonotonously behavior of the beam waist width versus I_{RW}. For small values of I_{RW} the beam waist is narrow. With increasing current the beam waist width increases. However, even at higher currents there are also regions with a smaller beam waist width.

The crosses in Fig. 7(b) show the dependence of the beam waist width on the current for the case of common contacting. The dots represent the deduced data from the experimental results shown in Fig. 7(a). There is a strong correlation between the deduced data and the directly measured ones.

The experiments show that based on measurements with separated contacts the features of a tapered device with common contacts are predictable. Based on the assumption of a parallel connection of RW and tapered sections, not only the electrical properties, but also the beam parameters can be determined.

IV. CONCLUSION

In the experiments presented, the potential of tapered lasers with electrically separated RW and tapered sections has been investigated. For the epi-side up mounted diode lasers under study emitting at 980 nm output powers up to 14 W in quasi CW operation were measured.

For the separate contacting of RW and tapered sections and a suitably chosen current through the RW section at an output power of $P = 6.5$ W more than 70% of the power lies inside the central lobe and the beam propagation ratio is $M^2 \leq 1.2$. At an output power of 7.7 W still a good beam quality with a low value of $M^2 = 1.9$ was obtained. Thus, together with the low vertical divergence these devices have an excellent beam shape, which allows an effective coupling of the laser light into fibers.

The measurements of devices with separate contacting allow conclusions on the electro-optical properties of devices with common contacting.

ACKNOWLEDGMENT

The authors are grateful to P. Brade, D. Friedrich, and O. Bauer for their technical assistance.

REFERENCES

[1] J. N. Walpole, “Semiconductor amplifiers and lasers with tapered gain regions,” *Opt. Quantum Electron.*, vol. 28, pp. 623–645, 1996.

[2] B. Sumpf, R. Hülsewede, G. Erbert, C. Dzionk, J. Fricke, A. Knauer, W. Pittroff, P. Ressel, J. Sebastian, H. Wenzel, and G. Tränkle, “High-brightness 735-nm tapered diode lasers,” *Electron. Lett.*, vol. 38, pp. 183–184, 2002.

[3] G. Erbert, J. Fricke, R. Hülsewede, A. Knauer, W. Pittroff, P. Ressel, J. Sebastian, B. Sumpf, H. Wenzel, and G. Tränkle, “3 W—High brightness tapered diode lasers at 735 nm based on tensile strained GaAsP-QWs,” in *Proc. SPIE*: vol. 4995, Novel In-Plane Semiconductor Lasers II, C. F. Gmachl and D. P. Bour, Eds. Bellingham, WA, 2003, pp. 29–38.

[4] B. Sumpf, G. Beister, G. Erbert, J. Fricke, A. Knauer, P. Ressel, and G. Tränkle, “Reliable 1 W CW operation of high-brightness tapered diode lasers at 735 nm,” *IEEE Photon. Technol. Lett.* vol. 16, no. 4, pp. 984–986, Apr. 2004

[5] D. Mehuys, S. O’Brien, R. J. Lang, A. A. Hardy, and D. F. Welch, “5 W diffraction-limited, tapered-stripe unstable resonator semiconductor laser,” *Electron. Lett.*, vol. 30, pp. 1885–1856, 1994.

[6] M. T. Kelemen, J. Weber, F. Rinner, J. Rogg, M. Mikulla, and G. Weimann, “High-brightness 1040-nm tapered diode lasers,” in *Proc. SPIE Int. Symp. Photonics Fabrication Europe 2002*, vol. 4947B-29, 2002, pp. 252–260.

[7] B. Sumpf, R. Hülsewede, G. Erbert, C. Dzionk, J. Fricke, A. Knauer, W. Pttroff, P. Ressel, J. Sebastian, and G. Tränkle, “High brightness 735 nm tapered lasers—Optimisation of the laser geometry,” *Opt. Quantum Electron.*, vol. 35, pp. 521–532, 2003.

Katrin Paschke was born in Schwedt, Germany, in 1969. She received the Diploma degree in physics from University of Potsdam, Germany, in 1996. Since 1997, she has been working on noise and reliability of optoelectronical devices at Ferdinand-Braun-Institut für Höchstfrequenztechnik, Berlin, Germany, where she is working towards the Ph.D. degree.

Her research interests included modeling and design of the high-power α DFB laser, as well as device fabrication and characterization. Her current research activities are the analysis of high brightness tapered diode lasers.

Bernd Sumpf was born in Berlin, Germany, in 1958. He received the Diploma in physics and the Ph.D. degree from the Humboldt-Universität, Berlin, Germany, in 1981 and 1987, respectively, for his work on lead salt diode lasers for spectroscopic applications.

From 1993 to 1997, he worked at the Technische Universität, Berlin, Germany, on high-resolution spectroscopy and difference-frequency generation. In 1997, he received the postdoctoral lecture qualification. Since 2000, he has worked at the Ferdinand-Braun-Institut für Höchstfrequenztechnik, Berlin, Germany, on high power and high brightness diode lasers.

Frank Dittmar received the Diploma degree in physics from the Wilhelms-University, Münster, Germany, in 1996. In 2002, he joined the Ferdinand-Braun-Institute and is currently pursuing the Ph.D. degree.

Until 1997, he continued working on stabilized tunable diode lasers and spectroscopy. From 1997 to 2002, he worked on electron probe micro analysis with an EDS manufacturer. His research interests include the design optimization of high-power taper lasers and the characterization of their beam quality.

Götz Erbert (M’95) received the diploma and doctoral degrees in physics from Humboldt-University, Berlin, Germany, in 1973 and from the Academy of Sciences of the German Democratic Republic (GDR) in 1990, respectively.

From 1973 to 1991, he worked at the Academy of Sciences first on integrated optics, dynamic holographic gratings in semiconductors and later on semiconductor lasers. In 1992, he joined the Ferdinand-Braun-Institut für Höchstfrequenztechnik, Berlin. Since 1996 he has been responsible for the optoelectronic activities in the institute. He is working on high-power semiconductor lasers based on GaAs using strained-layer quantum-well active regions in the wavelength range from 650 to 1200 nm.

Ralf Staske studied physics at the Humbold-University, Berlin, Germany, and received the Diploma degree in 1979.

From 1979 to 1991, he worked at the Academy of Sciences of the German Democratic Republic (GDR) in the field of photoluminescence on semiconductor layers. Since 1992 he has been with the Ferdinand-Braun-Institut für Höchstfrequenztechnik, Berlin, where he dealt with position detection in submicrometer range with a fiber optical sensor. Since 1996, he has worked at the field of electrooptical characterization of semiconductor lasers.

Hans Wenzel received the Diploma and Doctoral degrees in physics from Humboldt-University, Berlin, Germany, in 1986 and 1991, respectively. His thesis dealt with the electro-optical modeling of semiconductor lasers.

From 1991 to 1994, he was involved in a research project on the three-dimensional simulation of DFB lasers. In 1994, he joined the Ferdinand-Braun-Institut für Höchstfrequenztechnik, Berlin, where he is engaged in the development of high–power semiconductor lasers. His main research interests include the analysis, modeling, and simulation of optoelectronic devices.

Günther Tränkle (M'95) received the Diploma degree in physics from the Technical University of Munich, Munich, Germany, in 1981 and the Doctoral degree in physics at the University of Stuttgart, Stuttgart, Germany, in 1988.

In 1988, he joined the Walter-Schottky-Institute at the Technical University of Munich, running its III/V-semiconductor technology and working on field-effect transistors and laser diodes. From 1995 to 1996, he was a Department Head at the Fraunhofer-Institute for Applied Solid-State Physics, Freiburg, Germany, where he was responsible for the development and realization of electronic and optoelectronic III/V semiconductor devices, as well as quantum-well infrared detector arrays. In 1996, he became head of the Ferdinand-Braun-Institut für Höchstfrequenztechnik, Berlin. Since 2002, he has been chair on microwaves and optoelectronics at the Technical University of Berlin. His current research interests include III/V-technology, micro- and millimeter-wave transistors and circuits, GaN electronics, and high-power diode lasers.